

**Progress Report on Mesoporous Silica Nanoparticles for Drug Delivery**

*Miguel Manzano and María Vallet-Regí\**

Dr. M. Manzano, Prof. M. Vallet-Regí  
Departamento de Química en Ciencias Farmacéuticas, Facultad de Farmacia, Universidad Complutense de Madrid, Instituto de Investigación Sanitaria Hospital 12 de Octubre i+12, Plaza Ramón y Cajal s/n, 28040 Madrid, Spain.

Dr. M. Manzano, Prof. M. Vallet-Regí  
CIBER de Bioingeniería, Biomateriales y Nanomedicina, CIBER-BBN, Madrid, Spain.

E-mail: vallet@ucm.es

**Keywords:** mesoporous silica nanoparticles, smart drug delivery, targeting, biomedical applications

**Abstract**

In recent years, nanomedicine has emerged at the forefront of nanotechnology area generating great expectations in the biomedical field. Researchers are developing novel nanoparticles for both diagnostic applications using imaging technology and treatment purposes through drug delivery technologies. Among all the available nanoparticles, inorganic mesoporous silica nanoparticles are the newcomers to the field contributing with their unique and superlative properties. In this Progress Report we provide a brief overview of the most recent progress in the synthesis of mesoporous silica nanoparticles and their use as drug delivery nanocarriers. This contribution also updates the last trends on this type of nanoparticles towards their use in modern medicine highlighting the significant impact that this technology might have in the near future.

**1. Introduction**

Mesoporous Silica Materials (MSMs) were first reported by Kuroda *et al.* in Japan and the Mobil Oil scientists in USA back in the 1990s.<sup>[1],[2]</sup> Bulk mesoporous materials are produced employing self-assembled surfactant molecules as templates for condensation the silica

precursors around them. Then, removing the template leads to a material full of network cavities. This new family of materials is characterized by an ordered distribution of the pores that present homogeneous sizes between 2 and 20 nm, high pore volume (*ca.* 1 cm<sup>3</sup>/g), great surface area (*ca.* 1000 m<sup>2</sup>/g) and high density of silanol groups at their surface, that might favor subsequent functionalization processes. These features made MSMs ideal candidates for applications that might require the adsorption of molecules, such as drug delivery systems, as proposed by the Vallet-Regí group for the first time back in 2001.<sup>[3]</sup>

Additionally, MSMs are a type of mesostructured bioceramics that have shown bioactive behavior<sup>[4]</sup> thanks to the presence of silanol groups at their surface and a similar chemical composition to bioactive glasses.<sup>[5]</sup> Consequently, MSMs have been employed as starting materials for the manufacture of 3-D scaffolds for bone tissue engineering (Figure 1).<sup>[6]</sup>

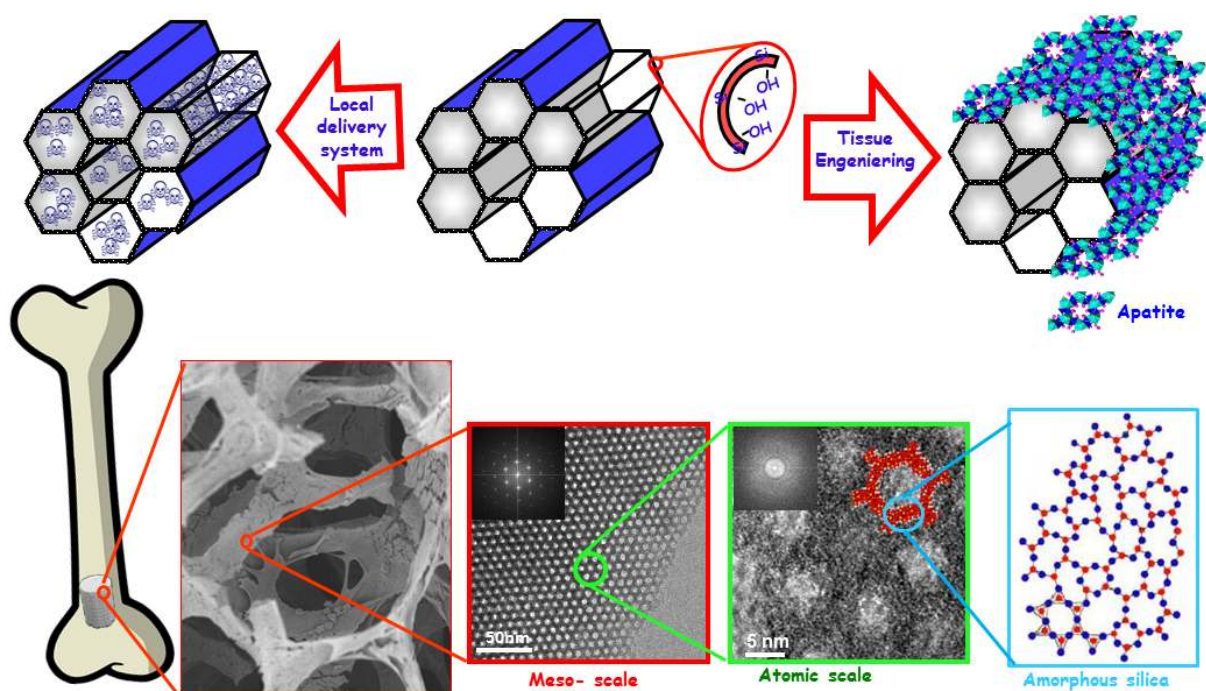


**Figure 1.** Top: schematic representation of the two main applications of mesoporous silica materials in biomedicine: drug delivery and bone tissue engineering. Bottom: Mesoporous Silica Materials are constituted of amorphous silica at atomic scale, with an ordered mesostructure that can be employed to manufacture 3D scaffolds with certain macroporosity

useful for bone tissue engineering. Adapted from reference <sup>[7]</sup> with permission from Walter de Gruyter and Company.

The great textural properties of bulk MSMs and their potential biomedical applications inspired their translation to the nanoscale dimension.<sup>[8]</sup> Thus, a few years later, mesoporous silica nanoparticles (MSNs) were developed and investigated as drug delivery systems by many research groups Worldwide.<sup>[9],[10],[11],[12],[13]</sup> Some of the major biomedical uses proposed for MSNs include cancer treatment, infectious treatment and different bone diseases.<sup>[14]</sup> Additionally, MSNs can also be used as effective imaging agents since many types of dyes and contrast agents can be incorporated into the pores of MSNs.<sup>[15]</sup>

The excellent properties of MSNs for biomedical applications have triggered the development of novel advanced multifunctional materials for a broad range of biotechnological applications. Among them, the last research breakthroughs in the biomedical area using MSNs could represent some of the cornerstones for future personalized treatments and diagnostic techniques with outstanding selectivity. In this sense, the continuous advances in nanotechnology, including synthesis and characterization techniques, make possible to develop nanoparticles able to establish intimate interactions within the biological world. This Progress Report will focus on the recent developments of mesoporous silica nanoparticles and the last advances on their application in drug delivery technologies.

## 2. Preparation and properties of Mesoporous Silica Nanoparticles

Silica nanoparticles are composed of colloidal amorphous metal oxide that can be produced *via* the *sol-gel* method and present diameters between 50 and 300 nm. There is a variety of methods that can be used for the production of mesoporous silica nanoparticles but, in general terms, the synthetic route relies in three processes: the *sol-gel* process for producing silica, the use of surfactants as structure directing agents for producing mesoporous materials, and a

modification of the Stöber method under dilute conditions to yield spherical nanoparticles.

[10],[16],[17],[18]

Silica nanoparticles are conventionally produced through the hydrolytic *sol-gel* process involving the hydrolysis and condensation of silicon alkoxide precursors under acidic or basic catalysis. As polycondensation takes place around the surfactant molecules that act as a template of the structure, the precursors form an oxide network that leads to a colloidal solution, *sol*, that gradually evolves towards the formation of a *gel* or discrete particles, depending on the conditions.<sup>[19]</sup> Using very dilute conditions allows obtaining monodispersed spherical silica particles.<sup>[20]</sup> Figure 2 illustrates the synthetic path in which the surfactant is initially dissolved in water at basic pH. The type of surfactant together with concentration and temperature would have a strong influence on the self-assembling process and, consequently, on the final mesostructure of the material. Then the silica precursor is added dropwise ensuring dilute concentration of the silica precursors. After the *sol-gel* process takes place, the droplets would gradually transform into nanoparticles. Then, the surfactant template is removed through solvent extraction leading to mesoporous nanoparticles made of pure silica.

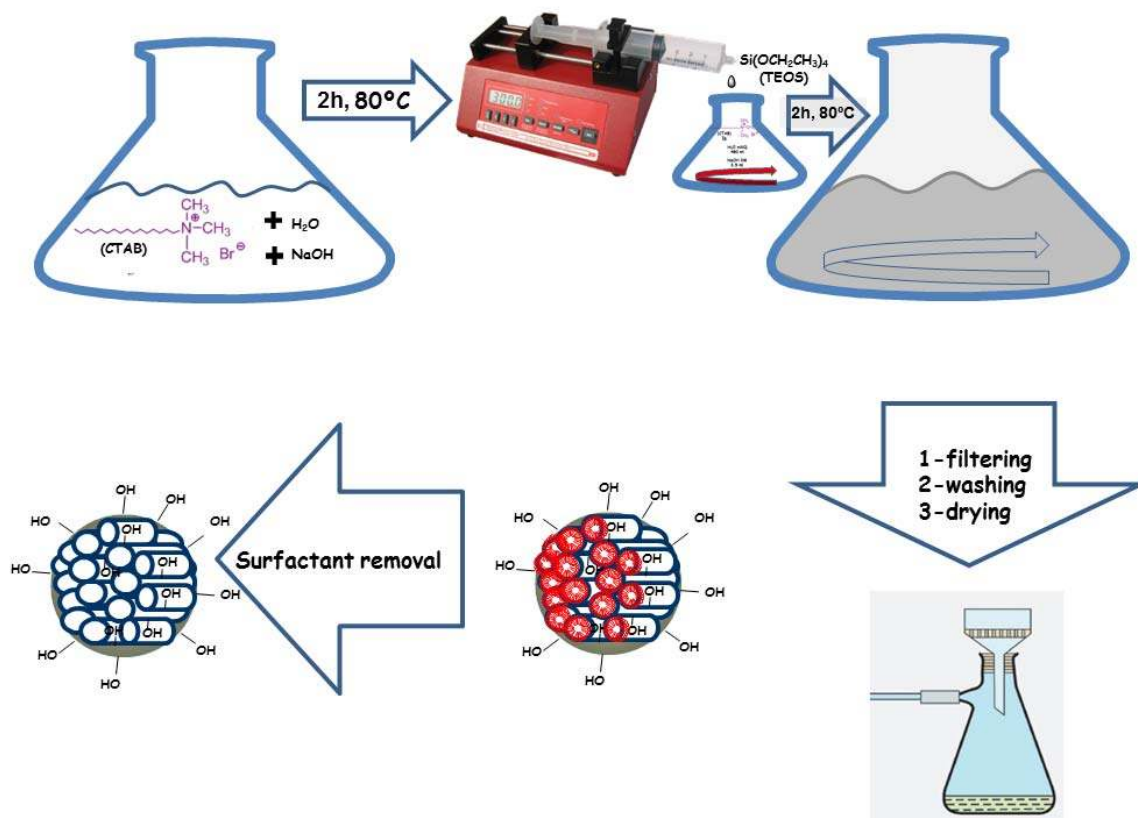


**Figure 2.** Synthetic path for the synthesis of MSNs in which the surfactant molecules are initially dissolved in water to then add dropwise the silica precursor that would condensate around the surfactant template. Then, after the *sol-gel* process takes place and the silica nanoparticles are formed, the surfactant removal leads to monodispersed spherical MSNs.

### 3. Properties of Mesoporous Silica Nanoparticles

Mesoporous Silica Nanoparticles present well-defined and tunable physicochemical properties, including particle size, pore size, pore volume, surface area, volume area, pore structure and surface functionality. The porous structure of mesoporous silica materials provides cavities that can host and release a great variety of biomolecules and therapeutic agents. In fact, the versatility of MSNs in size, morphology and texture has fueled their application as controlled drug delivery nanocarriers.<sup>[21]</sup> In this sense, MSNs can be produced with different particle diameters, different pore diameters, different porosity (parallel channels or radial pores), with



magnetic nanoparticles embedded into their skeleton or even growing the mesoporous network from different metal nanoparticles cores (Figure 3).

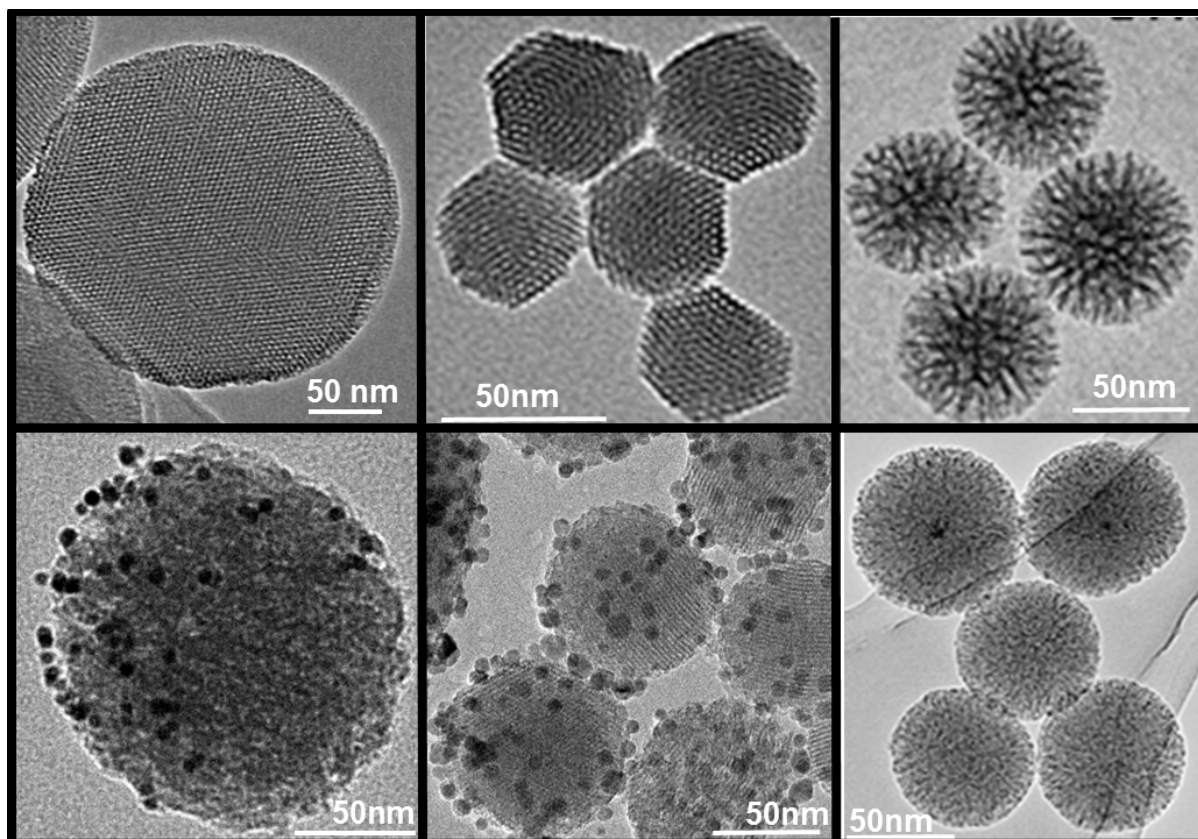


**Figure 3.** Transmission Electron Microscopy images of different MSNs with diverse size, morphology, composition and mesostructure. 1<sup>st</sup> row: longitudinal or 2D-hexagonal MSNs with different particle diameter (150 and 50 nm), MSNs with center radial porosity. 2<sup>nd</sup> row: Janus MSNs nanoparticles coated with gold nanoparticles, MSNs coated with magnetite nanoparticles and magnetite nanoparticles as core of MSNs. Adapted from reference [22] with permission from Taylor & Francis Academic Journal.

The particle diameter can be tuned depending on the synthetic conditions, ranging from few micrometers down to few nanometers. Regarding their use as drug delivery nanocarriers, monodisperse nanoparticles can be prepared with sizes relevant in biological environments, from 300 to 10 nm. In this sense, the particle size should be optimized for each specific biomedical application.<sup>[23]</sup>

The pore size of MSNs is a limiting factor of the molecules that could be introduced into the mesopores in terms of size. The pore diameter can be tuned from 2 to 30 nm depending on the surfactant employed as template and the synthesis conditions employed. In this sense, MSNs with large pore diameters (up to 50 nm) are employed for the adsorption and delivery of proteins, enzymes, antibodies and nucleic acids, as reviewed by Knezevic *et al.*<sup>[24]</sup>

The pore volume of conventional MSNs is *ca.* 1 cm<sup>3</sup>/g, although Haynes *et al.* have been able to increase it up to 4.5 cm<sup>3</sup>/g.<sup>[25]</sup> The pore volume is an important factor determining the amount of cargo molecules that can be loaded, and MSNs are well known because of the great amount of molecules that can host in their network of cavities. Taking into account that drug loading is a surface phenomenon, the high surface area of MSNs ensures the great loading capability of this type of nanocarriers, as it has been mentioned above, sometimes even exceeding 35 wt.%.<sup>[26]</sup>

Different porous morphologies and textures for MSNs have been reported, such as MCM-41-like hexagonal, cubic, concentric, foam-like, radial, or worm-like porosity. In fact, it has been reported that controlling the morphology of the MSNs pores permits to selectively load different molecules of various sizes and, similarly, tune the cargo release together with the matrix dissolution kinetics.<sup>[23]</sup>

As it has been mentioned above, adsorption is a surface phenomenon that is strongly influenced by the potential host-guest interaction. In this regard, the chemistry of the surface of MSNs could be easily tuned thorough the functionalization of the silanol groups located at the surface of the matrices. The literature has described many surface modification strategies to covalently attach almost any functional group.<sup>[27]</sup> Thus, the host-guest interaction can be designed as desired allowing the engineering of versatile nanocarriers.

#### 4. Safety and Biodegradation of MSNs

Despite all the scientific publications and interest on mesoporous silica nanoparticles, MSNs have not been approved by the Food and Drug Administration (FDA) for use in medical applications. To achieve that, it is important to address the possible biodistribution, clearance routes and the final fate of these nanoparticles in the body.<sup>[28]</sup> In general, the performance of any material is dependent on the rate and extent of Adsorption, Distribution, Metabolism and Elimination (ADME). From the nanotechnology point of view, those processes are included into biokinetics, which include uptake, biodistribution and elimination.<sup>[29]</sup>

The most common routes of administration of nanoparticles for drug delivery are intravenous, subcutaneous, and intratumoral injections. The benefits of injecting the nanoparticles into the blood stream include the rapid delivery and distribution throughout the vasculature. However, the stability of those nanoparticles in physiological media is an important requirement to use them through the bloodstream. In this sense, it is very important that the nanocarriers might be robust enough from the chemically point of view to protect the loaded cargo during the journey. Then, it could also be desirable that the carriers might degrade upon accomplishing their mission. Therefore, it is essential to understand the potential lixiviation rate of MSNs in physiological fluids to control the release kinetics and the cytotoxicity. MSNs consist of a SiO<sub>2</sub> matrix that could be susceptible to nucleophilic attack by OH from water in aqueous media, leading to the hydrolytic breakdown of the network and orthosilicic acid as by-product, which is biocompatible and excreted through the urine. In this sense, the degradability of MSNs is governed by the dissolution mechanism of silica particles into silicic acid in biological media.<sup>[23]</sup> This acid is soluble in water and contributes to maintain bone health, so silica has been recognized as safe by the FDA for over 50 years.<sup>[21]</sup> The dissolution rate of MSNs depends on the particle characteristics (such as surface area, pore size, condensation degree, functionalization, etc.) and on the degradation medium characteristics (pH, temperature, concentration, etc). Thus, the dissolution of MSNs can be tuned from few hours to several



weeks, depending on the final application. In this sense, the incorporation of different additives, both organic or inorganic, can modify the dissolution rate of MSNs. Examples include the noncovalent incorporation of organic molecules, such as photosensitizers<sup>[30]</sup> or anticancer drugs,<sup>[31]</sup> or inorganic moieties such as zirconium,<sup>[32]</sup> calcium,<sup>[33]</sup> manganese or iron.<sup>[34]</sup> On the other hand, the covalent incorporation of organic moieties has not only modified the degradation kinetics of MSNs, but has created a new category of mesoporous nanoparticles so-called periodic mesoporous organosilicas (PMOs).<sup>[35]</sup> This new type of materials share similar synthetic protocols and framework with MSNs, but they can offer totally different properties, including degradation rates, thanks to the great versatility of different organic molecules that can be introduced within the mesostructure. Thus, PMOs could be quite relevant for future clinical applications of mesoporous silica nanoparticles.<sup>[23]</sup> In this sense, different organic moieties were found to protect the mesoporosity for long periods of time,<sup>[36]</sup> as many studies on degradation kinetics have demonstrated, such as ethylene-curcumin-bridged PMS nanospheres,<sup>[37]</sup> ethylene-bridged PMO with a rod-like morphology<sup>[38]</sup>, phenylene-bridged PMO nanospheres,<sup>[39]</sup> and other degradable organic derivate that have been incorporated into PMOs.<sup>[21]</sup> Among them, cleavable organic moieties such as disulfide,<sup>[40]</sup> tetrasulfide,<sup>[41]</sup> oxamide<sup>[42]</sup> and lysine<sup>[43]</sup> have been incorporated within the framework of PMO nanoparticles for tuning the degradability kinetics on demand.

The *in vitro* degradation process on MSNs in relevant physiological media has been previously investigated,<sup>[44]</sup> finding that the intrinsic characteristics of MSNs remain stable long enough to guarantee their functionality as drug delivery nanocarriers. As commented above, the main factors governing the MSNs degradation under relevant physiological conditions were found to be the surface area, morphology, the chemical composition (potential functionalization of the nanoparticles surface) and the loaded cargo, among others.<sup>[45]</sup> On the other hand, the *in vivo* dissolution or biodegradation of MSNs has been analyzed with different animal models and, in

most of the cases, the surface functionalization of the nanoparticles with polymeric coatings has improved the stability and increased the bloodstream circulation time.

The biodistribution of MSNs has been explored only in small animals, confirming the MSNs accumulation in the reticuloendothelial system (RES), which include lungs, liver, and spleen.<sup>[46]</sup> That accumulation into the RES organs has been attributed to the adsorption of serum proteins onto nanoparticles, and this is why MSNs have been typically functionalized with hydrophilic polymers like poly(ethylene glycol) (PEG). However, it has recently been found that those adsorbed proteins can somehow enhance the cellular selectivity of targeted MSNs,<sup>[47]</sup> which is indicative that the composition of the protein corona can influence the biodistribution of the nanoparticles. In this sense, the required surface modification of MSNs would also influence on the protein corona and, consequently, on the biodistribution of those nanoparticles in comparison to unmodified MSNs.

Biodistribution of MSNs has been evaluated after radiolabeling MSNs with positron emission tomography (PET) detectable <sup>64</sup>Cu using BALB/c mice bearing xenografts of murine breast cancer tumors<sup>[48]</sup> and nude mice bearing xenografted human glioblastoma tumors.<sup>[49]</sup> The biodistributions were observed to be similar in both approaches regardless of the presence of a targeting ligand or not. The liver presented the highest concentration of nanoparticles while low MSNs concentration was observed in lung, spleen, kidney and intestines. Additionally, the particle concentration in the blood remained relatively low. These studies demonstrated almost identical biodistribution independently of the different animal models employed. Similar biodistribution experiments with different labelling elements such as <sup>89</sup>Zr and <sup>45</sup>Ti with different particle diameter led to the conclusion that increasing particle size from 80 to 160 nm promoted higher accumulation in the spleen than in the liver.<sup>[50][51]</sup> Same size of MSNs (80 nm) but different labelling (fluorescent dye) were employed for evaluating the biodistribution on tumor-free mice.<sup>[52]</sup> In this case, the highest amount of MSNs was found in the spleen, but particles were also observed in liver and lung. In that study, the effect of particle size and

functionalization on biodistribution was also evaluated. MSNs functionalized with PEG presented longer blood circulation time regardless of the particle size, as expected. However, larger nanoparticles presented much shorter blood circulation time, presumably because of their accumulation in the liver and the spleen. A similar effect of MSNs functionalized with PEG and labelled with  $^{89}\text{Zr}$  was observed in mice xenografted with LNCaP and PC-3 tumors. The non-PEGylated particles were rapidly accumulated in lung, liver and spleen while PEG-MSNs presented much longer blood circulation time.<sup>[53][54]</sup> When MSNs were functionalized with cationic species, such as amine groups, a quick accumulation in the liver was observed, which could be explained by the fast protein adsorption onto the cationic surface of MSNs.<sup>[55][56]</sup> Besides the size and surface functionalization, the particle shape has also shown a strong influence on the biodistribution of MSNs. In this sense, spherical and elongated MSNs have been studied, finding that elongated and cylindrical particles tend to accumulate in the spleen and present shorter blood circulation time as compared to spherical particles.<sup>[55][57][58]</sup> Regarding the clearance of MSNs from the body, different studies have confirmed that renal elimination is the main excretion route for this type of nanoparticles.<sup>[23][57]</sup> Among those studies, a seminal investigation by Tamanoi and coworkers demonstrated that MSNs were initially observed in the spleen and in the liver, but most of them were renally excreted after 96 hours, with a minority being excreted through feces after that time, as observed in Figure 4.<sup>[59]</sup>

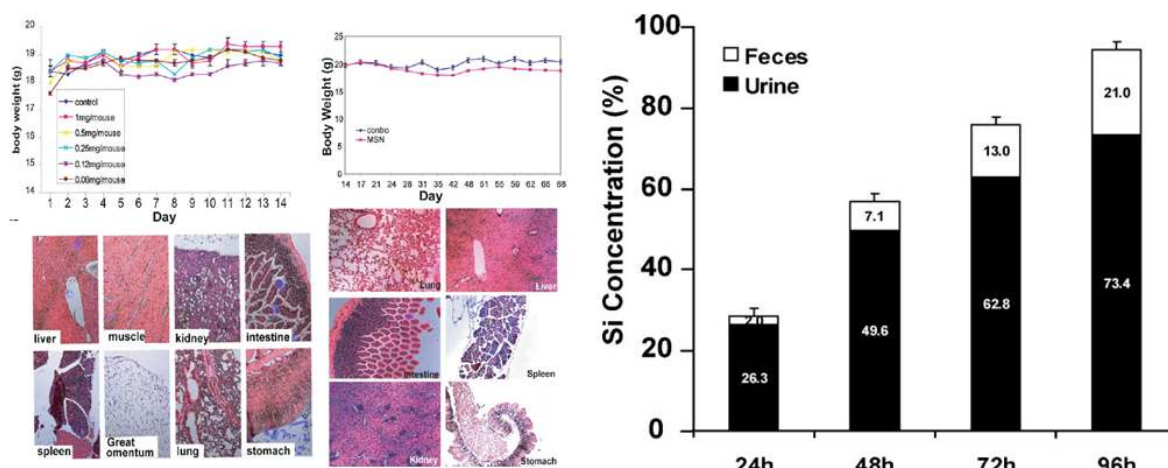


**Figure 4.** Toxicity evaluation of MSNs injected intravenously in 12 female mice twice per week for 14 days. Left: Top left corner: average body weights; bottom left corner: representative tissue sections of mice stained with hematoxylin and eosin; Top right corner: two groups of mice were administered MSNs at a dose of 1 mg per mouse or saline solution, in the plot the average body weights; bottom right corner: representative tissue sections of mice stained with hematoxylin and eosin. Right: analysis of the Si concentration in urine and feces of mice collected after injection of MSNs. Adapted from ref. <sup>[59]</sup> with permission from John Wiley and Sons.

Although partial particle dissolution was assumed to be necessary for renal clearance,<sup>[60]</sup> many reports have found intact MSNs with sizes larger than 90 nm in the urine,<sup>[57][59][61]</sup> and no mechanisms have been proposed for this observation.

Regarding other excretion routes, hepatobiliary excretion through the liver and bile is governed by protein adsorption<sup>[62]</sup> and excretion through the feces has been observed to be favored by aggregation of small particles.<sup>[63]</sup>

There is an interesting connection between the blood circulation time of MSNs and the excretion route.<sup>[64]</sup> The longer is the blood circulation time, typical for PEGylated MSNs, the slower is the clearance rate. Additionally, the PEG chains grafted on the surface of MSNs can slow their dissolution rate, which also helps to delay their clearance.<sup>[65]</sup>

#### 4. MSNs as smart drug delivery systems

The reasons for the great success of MSNs as drug delivery systems relies on their above mentioned physical-chemical properties. In fact, MSNs can provide a novel therapeutic armamentarium capable of addressing some of the main pitfalls of conventional medicine, such as the lack of drug specificity, the narrow window of efficacy of some medicines, the possible

low drug solubility and/or stability, adverse pharmacokinetic profiles and some possible side effects.

In general, any nanoparticle employed as a drug delivery system, should fulfill some basic requirements, as described in Figure 5, such as loading the maximum amount of cargo molecules, releasing the cargo on-demand avoiding premature release, reaching the diseased tissue to release the cargo only where needed and, in case of cancer treatment, penetrate deep into the tumor.

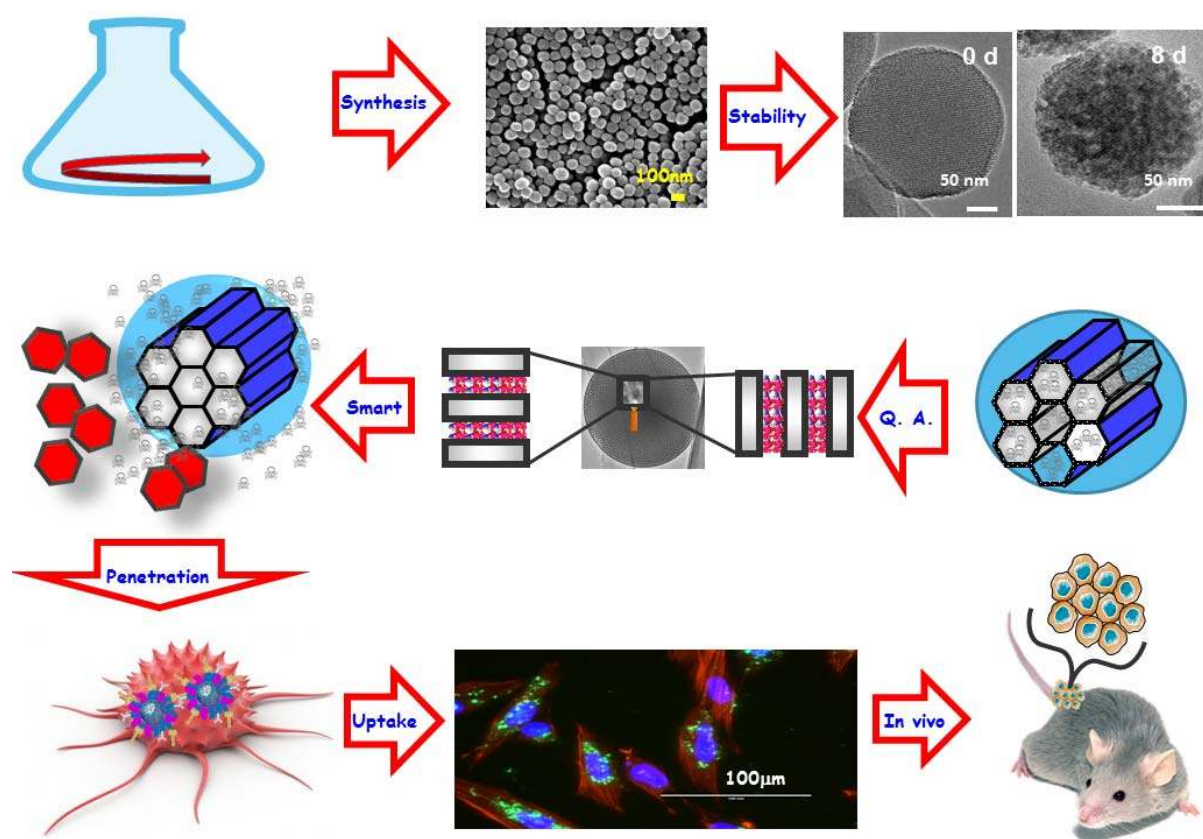


**Figure 5.** Representative roadmap for a MSNs platform to reach the preclinical studies, including the synthesis of the MSNs, demonstration of their stability, therapeutic cargo loading into the pores, Quality Assurance or characterization the loaded platform, smart release behavior, penetration into tumor mass, cellular uptake and *in vivo* evaluation. Adapted from reference <sup>[66]</sup> with permission from Elsevier.

#### 4.1 Loading and protecting the therapeutic cargo

There are two different ways of loading drugs into MSNs, *in situ* during the synthetic path or post-sorption (physisorption or chemisorption).<sup>[15]</sup> One of the benefits of the later is that involves a separate step following particle synthesis, which allows independent optimization of loading conditions. The most common approaches involve physical adsorption from solution into the mesopores, physical adsorption from solution onto the outer surface and covalent grafting. In any case, the high surface area and pore volume of MSNs ensure higher drug loadings than other type of nanoparticles, as mentioned above. This allows using fewer nanoparticles of MSNs than other nanocarriers for the potential treatment of the same disease, which might be of importance regarding potential toxicity issues.

An additional benefit of using MSNs as drug carriers is that cargo molecules loaded inside the mesopores will be protected from tough environmental factors within living systems such as enzymatic degradation or harsh pH. In fact, silica is an inorganic compound that can provide efficient protection of different types of encapsulated molecules.<sup>[67]</sup> Up to 2010, the location of cargo molecules in mesoporous materials was deduced from the sum of indirect techniques, such a nitrogen adsorption, Fourier transformed infrared spectroscopy, X-ray fluorescence spectroscopy, elemental analysis and/or thermogravimetry. However, the use of electronic microscopy allowed the direct evidence of the drug confinement into the inner part of the pore channels back in 2010.<sup>[68]</sup> Scanning Transmission Electron Microscopy (STEM) with spherical aberration correctors incorporated permitted the determination of the chemical composition of matrix network and pores (Figure 6). This microscopy technique is based on scanning the material with an electron probe that can be focused down to 1 nm or less on the sample. Afterwards, the STEM images can be formed with the collected scattered electrons in each probe position by the high-angle annular dark-field detector in synchronism with the scanning probe. This technique enables to perform analyses with enough resolution capable of atomic level analyses, which allowed us to distinguish between the pore wall (silica matrix) and the



pore space where the cargo molecules are confined. Consequently, this technology allowed for the first time the confirmation that the cargo molecules were actually into the inner area of the mesopores.

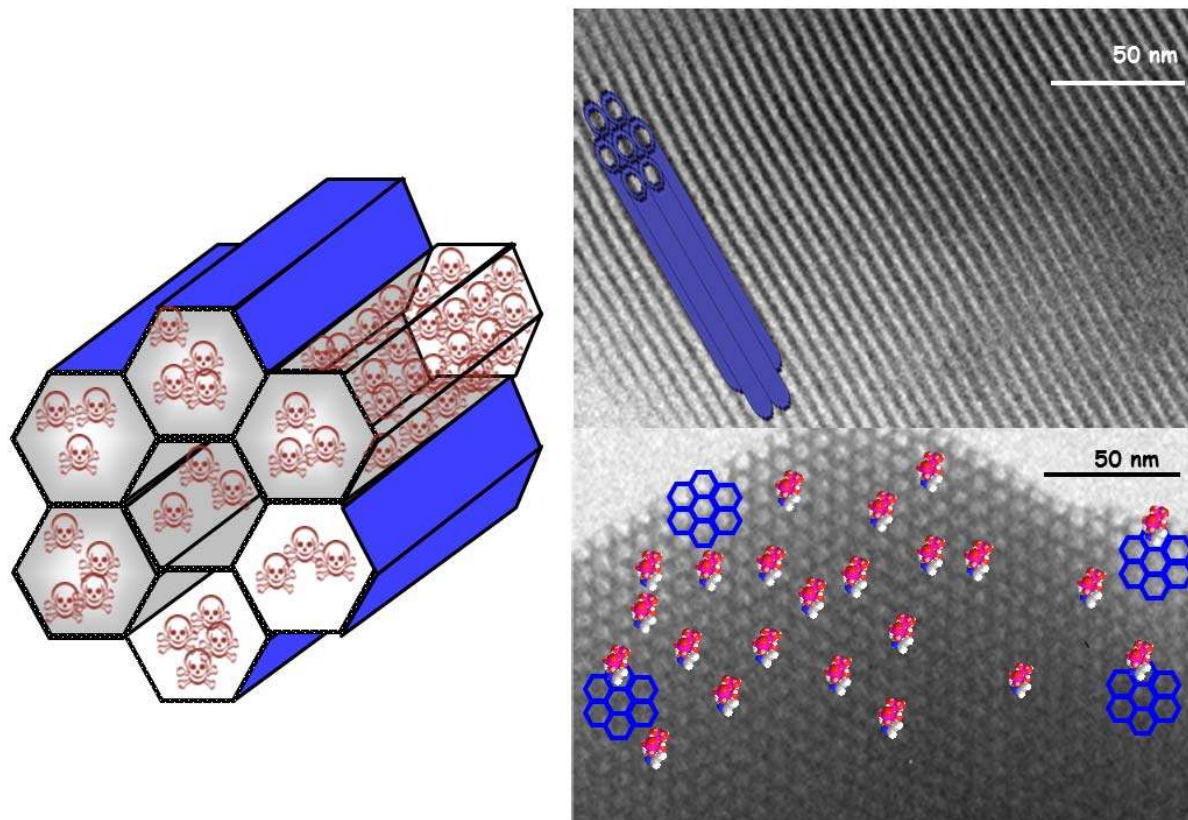


**Figure 6.** Schematic representation of the different possibilities for drug delivery technologies offered by MSNs (left), and Transmission Electron Microscopy images of MSNs from different perspectives where silica wall and mesopores (top right) and drug loaded pore entrances (bottom right) can be observed. Adapted from reference <sup>[68]</sup> with permission from the Royal Society of Chemistry.

#### 4.2 Release therapeutic cargo on-demand

An ideal nanocarrier should be able to release high local concentrations of the therapeutic cargo on-demand after the application of a stimulus, leading to smart drug delivery systems.<sup>[69]</sup> One of the advantages of this type of systems is that it is possible to avoid the premature release of

the transported cargo before reaching the targeted tissues, which improves the nanomedicine efficiency and reduces potential side effects if the cargo might be cytotoxic.

This stimuli-responsive approach is of particular interest for MSNs because of their peculiar and unique textural characteristics. It is relatively easy to introduce a therapeutic cargo inside the mesopores of MSNs, although it might also be very easy for those cargo molecules to diffuse out of the mesoporous channels. It is then necessary to close the pore entrances with a cap once the cargo is loaded inside the mesoporous network of cavities. The pore diameter of MSNs allows using large molecules to block the pore entrances. Only upon the application of certain stimuli, those cap agents would detach from the pore entrances triggering the cargo on-demand. Those capping systems can be divided into three main groups: reusable caps, based on a bulky capping molecule able to bind reversibly; completely reversible caps, based on the principle of reversal affinity of a ring shaped macromolecule into a steam with two or more binding sites; and, irreversible caps, based on a chemical bond cleavage of the capping molecule which leads to a permanent separation from the pore entrance of the MSN.<sup>[70]</sup>

There are two main types of stimuli that have been widely employed for triggering the therapeutic cargo release from MSNs: internal and external stimuli, as it can be observed in Figure 7.<sup>[13],[71],[72],[73],[74],[75],[76],[77],[78],[79],[80]</sup>

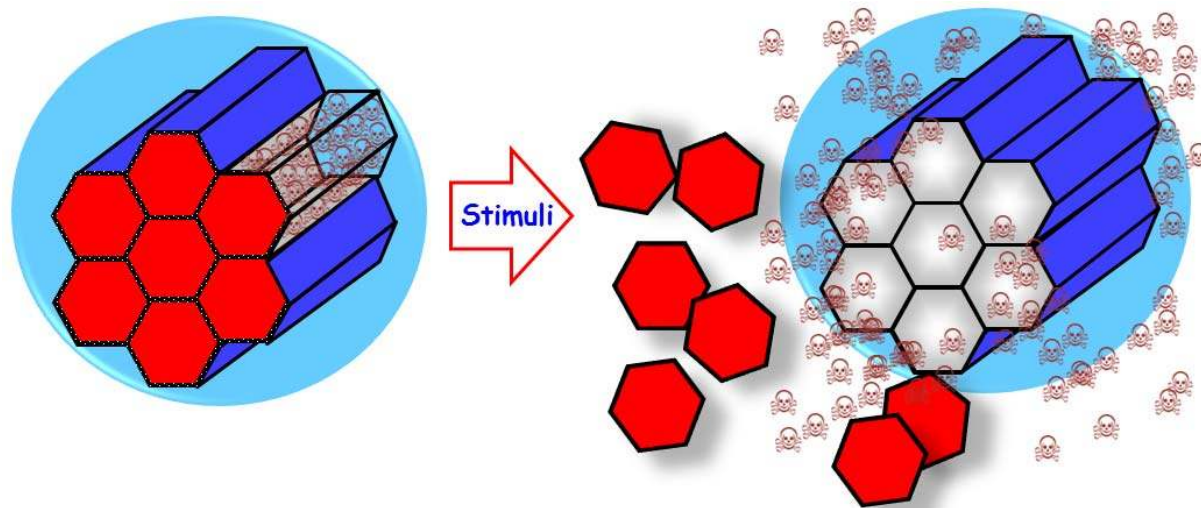


**Figure 7.** Schematic representation of stimuli-responsive MSNs that can be triggered with both internal or external stimuli to release the therapeutic cargo. Adapted from reference [7] with permission from Walter de Gruyter and Company.

Internal stimuli are those typical of the treated pathology, and the subsequent responsive MSNs are able to respond to chemical variations that take place in certain sites of the human body as a consequence of the differences between diseased and healthy organs and/or tissues.

Among the internal stimuli, pH is probable the most widely employed internal stimulus to trigger the cargo release from MSNs.<sup>[81],[82],[83],[84],[85],[86],[87],[88],[89],[90],[91],[92]</sup> The reason for that is because there are several pathologies that present different pHs than those of healthy conditions, such as extracellular pH of tumor tissues or the pH of inflamed tissues. There are also differences on the pH values inside the cells, depending on the cell compartment or organelle. The dysregulation of certain enzymes and/or specific antibodies, both hypo- or overexpression, in certain pathological states or diseased tissues can also be used for triggering the therapeutic cargo release from MSNs.<sup>[93],[94],[95],[96],[97],[98],[99],[100],[101],[102]</sup> Similarly, the change in redox potential as it happens in tumor tissues where the glutathione concentration can be four times higher than in healthy tissues, can be employed to develop responsive MSNs.<sup>[10],[103],[104],[105],[106],[107],[108],[109],[110],[111],[112]</sup>

On the other hand, external stimuli are those that can be activated remotely by the clinician, who is under control at all times. One of the benefits of this type of responsive nanocarriers is that the release can be turned on and off as required, which might lead to pulsatile responsive release systems. Additionally, some stimuli can be applied locally into the site of the disease, which increase the precision of the treatment improving the efficacy and efficiency.

The use of magnetic fields for triggering the cargo release from MSNs has been very popular because they allow magnetic guidance under a permanent magnetic field or temperature increase upon the application of an alternating magnetic field. This permits developing MSNs with a wide range of possibilities in the biomedical field. [9],[113],[114],[115],[116],[117],[118],[119],[120]

Ultrasounds is also an external stimulus that constitutes an efficient element for developing responsive MSNs with spatiotemporal control of the cargo delivery at the target site and preventing the damage of the healthy tissues. [121],[122],[123],[124],[125] Some of the benefits of Ultrasounds include its non-invasiveness, the absence of ionizing radiations and the easily regulation of tissue penetration depth by tuning some basic parameters.

Light also constitutes a useful alternative for developing externally triggered MSNs with non-invasive and spatiotemporal control of the release. [126],[127],[128],[129],[130],[131],[132],[133],[134] In this case, the wavelength of the radiation can be selected from different regions, such as ultraviolet, visible or near infrared (NIR). Some of the advantages of using light as stimulus relies on its easy application, low toxicity and precise focalization at the targeted tissue. However, the major pitfall relies on the low tissue penetration capability, which forces to use medical devices as those used for laparoscopic surgery. A possible alternative could be the use of two-photon-excited nanomedicine in the NIR, which allow imaging and therapy of small tumors that might be detected at an early stage. In fact, many cancers could be targeted using two-photon excitation strategies, such as retinoblastoma, prostate cancer, breast cancer or colon cancer. [135] Since the first drug delivery system based on MSNs for two-photon adsorption using coumarin as the provider of sufficient two-photon sensitivity was developed, [136] the progress of chemistry

and physics has allowed many efficient two-photon absorbers and photosensitizers.<sup>[40][137]</sup> Subsequently, many different versatile two-photon-triggered systems based on MSNs have been designed for the delivery of reactive oxygen species, drugs and genes to efficiently kill cancer cells.<sup>[138][139][140][141][142][143][144]</sup>

### 4.3 Transporting the therapeutic cargo to the right place

One of the key aspects for a nanocarrier, regardless of the type of nanoparticles, is to transport huge loads of therapeutic molecules to precise locations in the body for disease treatments with enhanced efficacy and reduced side effects. In this sense, it should be compulsory to look at the biological behavior of MSNs taking into account their biocompatibility, biodistribution, biodegradability and clearance.

As it has been mentioned above, the biocompatibility of MSNs has been evaluated in many studies, and it was found that toxicity might depend on several characteristics, such as size, shape, surface chemistry and surface charge.<sup>[67]</sup> After many different studies investigating the effect of the size,<sup>[59],[52],[145],[146],[147]</sup> it was found that relatively small MSNs could be considered as potentially safe candidates for biomedical applications. Nanoparticles smaller than 10 nm would undergo fast renal clearance, while nanoparticles larger than 300 nm could provoke embolisms due to their possible aggregation into capillaries and alveoli.

The shape effect was also evaluated using rods and spherical MSNs,<sup>[57]</sup> finding that MSNs shape might have an strong influence in cell interaction and biodistribution. Although spherical MSNs have been traditionally employed in nanomedicine due to their relatively easy fabrication process, rod-like MSNs present different accumulation tissues, and cellular internalization.<sup>[58],[148]</sup>

The surface of MSNs governs the interaction of the nanoparticles with the physiological environment, so both the chemical composition and the surface charge are of capital importance. Regarding the composition, the toxicity of MSNs towards certain cell lines could be attributed

to surface silanolates and/or silica reactive oxygen species generation.<sup>[12]</sup> Generally, MSNs are decorated with non-toxic hydrophilic polymers such as PEG to increase the blood circulation time and to enhance the stability in physiological fluids. The PEG layer prevents the non-specific protein adsorption which could trigger the immune response. Additionally, the functionalization of MSNs with PEG helps to avoid particle aggregation, which is very important to ensure the biocompatibility of this platform.

Many different groups have investigated the biodistribution of MSNs in animal models. In this sense, MSNs with different sizes and PEG functionalities were injected in healthy mice observing that pegylation favored the blood circulation time as the particles escaped from phagocytosis.<sup>[52]</sup> Basically, MSNs and pegylated MSNs accumulated in the liver and spleen after intravenous administration into healthy animals.

Most of the research on MSNs for drug delivery has been focused on the potential treatment of cancer. Therefore, it is of capital importance that those nanocarriers might accumulate in tumor tissues to release their cargo in there. In this sense, it is well known that nanoparticles leak into tumor when injected into the blood stream. The reason for that preferential accumulation in the tumor tissue, also called *passive targeting*, can be found in the particular blood vessel architecture of the tumor, which present wide fenestrations. Furthermore, tumor tissues usually lack effective lymphatic drainage, and this is why this preferential accumulation phenomenon is known as Enhanced Permeability and Retention (EPR) effect.<sup>[149]</sup> This effect has been exploited to increase the preferential accumulation of MSNs in mice affected by human cancer xenografts.<sup>[59],[150],[151],[56]</sup>

However, in certain cases the EPR effect offers smaller nanoparticle accumulation than initially expected, which might result in therapeutic concentrations that might not be good enough for treating some cancers.<sup>[152]</sup> A potential alternative to increase the nanoparticle accumulation into tumor tissue consists on decorating the surface of the nanoparticles with certain ligands that might present high affinity towards certain membrane receptors overexpressed in tumor



cells.<sup>[153]</sup> This targeting strategy, known as *active targeting*, has been employed by several research groups to increase the accumulation of MSNs into tumors using, among others, folate or peptides as targeting agents.<sup>[154],[61],[155],[156],[157],[139],[48]</sup> In this sense, it has been found that the combination of both passive and active targeting produce much better results in terms of therapeutic cargo selective accumulation when employed together. Figure 8 describes **the work for developing** a novel targeting agent for the **selective treatment of neuroblastoma**, which is the most frequent extra cranial pediatric tumor.<sup>[158]</sup> The combination of active and passive targeting approaches ensured a significant accumulation within the tumor mass after 48 and 72 hours of administration.

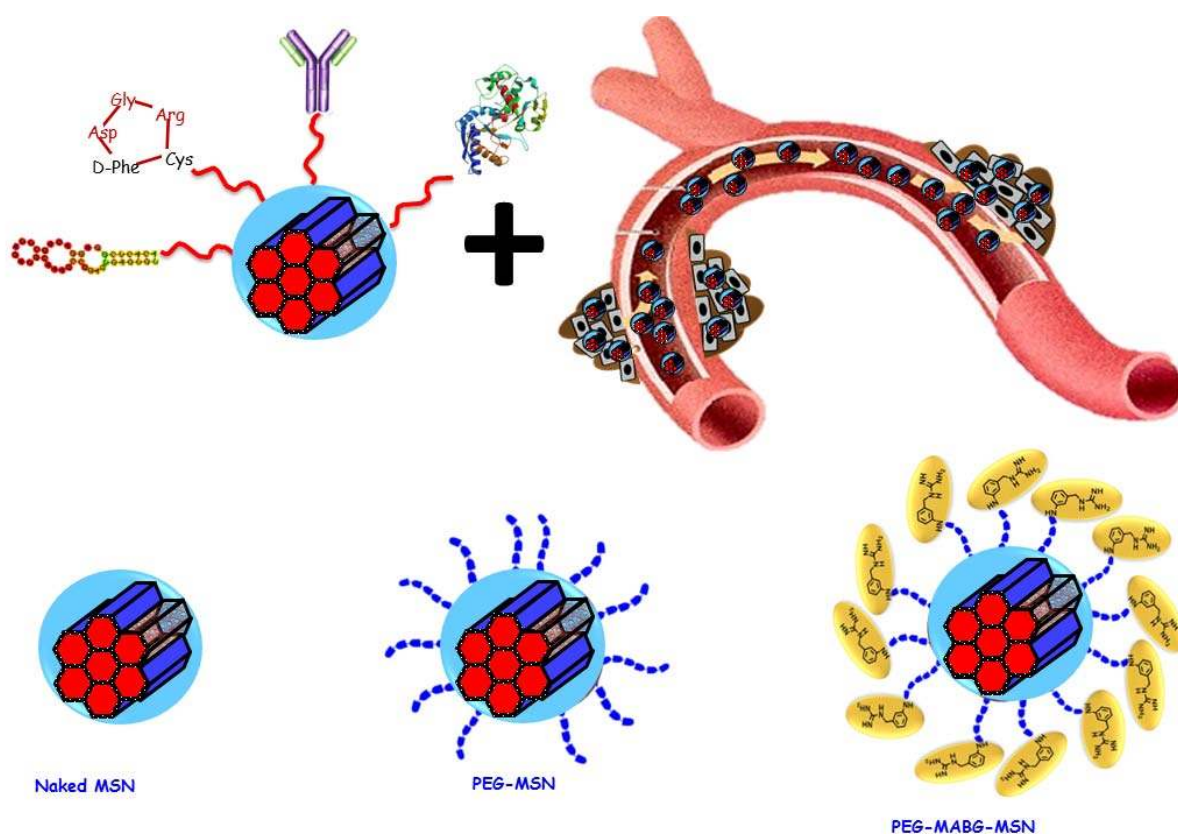


**Figure 8.** Schematic representation of the combination of active and passive targeting approaches (top) and the subsequent nanocarriers accumulation into tumor tissue resulting from that targeting combination using MSNs for the treatment of neuroblastoma (bottom).

It is also possible to develop a multi-targeted delivery system in terms of targeting tissues and cells with the same platform. In this case, the cell-organelle targeting might be of interest for the treatment of multidrug resistant tumors. MSNs technology permits developing a multifunctional two-drug double vectored nanocarriers through the assembly of different layers of functional building blocks. This system allows a sequential cell-organelle targeting of two different therapeutic cargoes.<sup>[159]</sup> A similar double-targeting approach was used for the diagnosis and treatment of neuroblastoma.<sup>[160]</sup> In this case, a family of novel scaffolds with structural analogues of meta-iodo-benzilguanidine, which presents a strong affinity towards norepinephrine transporter overexpressed on the membrane of neuroblastoma cells.

#### 4.4 Tumor penetration

Once the nanocarriers might have reached the targeted tissue of a solid tumor thanks to both passive and active targeting, they would find an additional problem. Tumor mass is normally constituted of a mixture of cancer cells, blood vessels and dense extracellular matrix. The high density of that matrix, normally higher than in healthy tissues, together with the elevated interstitial pressure of solid tumors, hinders the penetration of the nanocarriers limiting their therapeutic efficacy to the peripheral sites of the tumor.<sup>[161]</sup> A potential solution that has been explored is based on using proteolytic enzymes attached to the surface of nanoparticles to degrade the tumor matrix and, therefore, open the way to the nanocarriers to reach deeper areas of the tumor.<sup>[162]</sup> However, those enzymes could suffer from degradation during their way to the tumor, so it is possible to develop MSNs with protected proteolytic enzymes grafted at their surface. The designed platform was based on acid-degradable nanocapsules of collagenase that were formed with a pH-degradable cross-linker. Thus, when exposed at acid pH, which are typical from tumor tissues as a consequence of lactic acid accumulation, the enzymatic protection was degraded and the enzyme exposed powering the penetration deep into the tumor tissue.<sup>[163]</sup> In a totally different approach, ultrasound-induced inertial cavitation has been

recently evaluated as a mechanism to induce MSNs extravasation and penetration to a tumor mass.<sup>[164]</sup> Using an in vitro flow-through agarose tissue phantom MSNs were observed to extravasate into the agarose gel when Ultrasound was applied at pressures beyond the internal cavitation threshold, which could be applied to a real tumor tissue in the near future.

## 5. Conclusions and Outlook

In this Progress Report we have revised the origins of mesoporous silica nanoparticles together with their synthetic protocols and properties that made them suitable to be used as drug delivery nanocarriers. These MSNs are unique nanoparticles that combine the chemical and physical stability of silica and the potential offered by the network of cavities from the mesoporous structure. In fact, the unique properties of MSNs, such as their great loading capability, their controllable particle size and shape, their suitability for an easy functionalization and their biocompatibility, have made them ideal candidates to be used as therapeutic nanocarriers.

Regarding the roadmap that MSNs should follow to reach clinical trials, from our point of view, there are some important challenges that need to be fulfilled before clinical translation can be achieved. Among others, it is important to standardize the production protocols to achieve reproducibility in the synthesis of MSNs; it is also very important that the produced nanoparticles should display the appropriated stability and dispersibility; any surface functionalization method should also be standardized before reaching the clinic. More importantly, more biodistribution studies of MSNs on different animal models should be carried out to be absolutely sure of what would be the final fate of the MSNs.

From a general perspective, it is evident that there has been a huge progress in the design and development of MSNs for biomedical applications, as we have reflected in this Progress Report. However, it is obvious that a large amount of work still needs to be done before clinical translation might be achieved.

## Acknowledgements

This work was supported by the European Research Council, ERC-2015-AdG (VERDI), Proposal No. 694160

## Conflict of interest

The authors declare no conflict of interest.

## References

- [1] T. Yanagisawa, T. Shimizu, K. Kuroda, C. Kato, *Bull. Chem. Soc. Jpn.* **1990**, *63*, 988.
- [2] C. T. Kresge, M. E. Leonowicz, W. J. Roth, J. C. Vartuli, J. S. Beck, *Nature* **1992**, *359*, 710.
- [3] M. Vallet-Regí, A. Rámila, R. P. Del Real, J. Pérez-Pariente, *Chem. Mater.* **2001**, *13*, 308.
- [4] I. Izquierdo-Barba, L. Ruiz-González, J. C. Doadrio, J. M. González-Calbet, M. Vallet-Regí, *Solid State Sci.* **2005**, *7*, 983.
- [5] L. L. Hench, *J. Mater. Sci. Mater. Med.* **2006**, *17*, 967.
- [6] M. Vallet-Regí, L. Ruiz-González, I. Izquierdo-Barba, J. M. González-Calbet, *J. Mater. Chem.* **2006**, *16*, 26.
- [7] M. Vallet-Regí, Bioceramics: from bone substitutes to nanoparticles for drug delivery. *Pure Appl. Chem.* **2019**, *91*, 687.
- [8] M. Vallet-Regí, E. Ruiz-Hernández, *Adv. Mater.* **2011**, *23*, 5177.
- [9] E. Ruiz-Hernández, A. Baeza, M. Vallet-Regí, *ACS Nano* **2011**, *5*, 1259.
- [10] C.-Y. Lai, B. G. Trewyn, D. M. Jeftinija, K. Jeftinija, S. Xu, S. Jeftinija, V. S.-Y. Lin, *J. Am. Chem. Soc.* **2003**, *125*, 4451.
- [11] J. Lu, M. Liong, J. I. Zink, F. Tamanoi, *Small* **2007**, *3*, 1341.
- [12] D. Tarn, C. E. Ashley, M. Xue, E. C. Carnes, J. I. Zink, C. J. Brinker, *Acc. Chem. Res.* **2013**, *46*, 792.
- [13] C. Argyo, V. Weiss, C. Bräuchle, T. Bein, *Chem. Mater.* **2014**, *26*, 435.
- [14] P. Mora-Raimundo, D. Lozano, M. Manzano, M. Vallet-Regí, *ACS Nano* **2019**, *13*, 5451.
- [15] J. M. Rosenholm, C. S. and M. Linden, Multifunctional Mesoporous Silica Nanoparticles for Combined Therapeutic, Diagnostic and Targeted Action in Cancer Treatment. *Curr. Drug Targets* **2011**, *12*, 1166–1186.
- [16] Q. Cai, Z.-S. Luo, W.-Q. Pang, Y.-W. Fan, X.-H. Chen, F.-Z. Cui, *Chem. Mater.* **2001**, *13*, 258.
- [17] C. E. Fowler, D. Khushalani, B. Lebeau, S. Mann, *Adv. Mater.* **2001**, *13*, 649.
- [18] R. I. Nooney, D. Thirunavukkarasu, Y. Chen, R. Josephs, A. E. Ostafin, *Chem. Mater.* **2002**, *14*, 4721.
- [19] C. J. Brinker, G. W. Scherer, *Sol-Gel Science: The Physics and Chemistry of Sol-Gel Processing*; Brinker, C. J.; Scherer, G. W. B. T.-S.-G. S., Eds.; Academic Press: San Diego, 1990.
- [20] W. Stöber, A. Fink, E. Bohn, *J. Colloid Interface Sci.* **1968**, *26*, 62.
- [21] J. G. Croissant, Y. Fatieiev, A. Almalik, N. M. Khashab, *Adv. Healthc. Mater.* **2017**,

- 1700831, 1700831.
- [22] R. R. Castillo, D. Lozano, B. González, M. Manzano, I. Izquierdo-Barba, M. Vallet-Regí, *Expert Opin. Drug Deliv.* **2019**, *16*, 415.
- [23] J. G. Croissant, Y. Fatieiev, N. M. Khashab, *Adv. Mater.* **2017**, *29*, 1604634.
- [24] N. Ž. Knežević, J.-O. Durand, *Nanoscale* **2015**, *7*, 2199.
- [25] S. M. Egger, K. R. Hurley, A. Datt, G. Swindlehurst, C. L. Haynes, *Chem. Mater.* **2015**, *27*, 3193.
- [26] V. Mamaeva, C. Sahlgren, M. Lindén, *Adv. Drug Deliv. Rev.* **2013**, *65*, 689.
- [27] F. Hoffmann, M. Cornelius, J. Morell, M. Fröba, *Angew. Chemie Int. Ed.* **2006**, *45*, 3216.
- [28] J. Bourquin, A. Milosevic, D. Hauser, R. Lehner, F. Blank, A. Petri-Fink, B. Rothen-Rutishauser, *Adv. Mater.* **2018**, *30*, 1704307.
- [29] E. Markovsky, H. Baabur-Cohen, A. Eldar-Boock, L. Omer, G. Tiram, S. Ferber, P. Ofek, D. Polyak, A. Scomparin, R. Satchi-Fainaro, *J. Control. Release* **2012**, *161*, 446.
- [30] S. Zhao, S. Zhang, J. Ma, L. Fan, C. Yin, G. Lin, Q. Li, *Nanoscale* **2015**, *7*, 16389.
- [31] X. Zhou, L. Chen, W. Wang, Y. Jia, A. Chang, X. Mo, H. Wang, C. He, *RSC Adv.* **2015**, *5*, 65897.
- [32] M. Colilla, M. Manzano, I. Izquierdo-Barba, M. Vallet-Reg, C. Boissière, C. Sanchez, *Chem. Mater.* **2010**, *22*, 1821.
- [33] H. P. Rim, K. H. Min, H. J. Lee, S. Y. Jeong, S. C. Lee, *Angew. Chemie Int. Ed.* **2011**, *50*, 8853.
- [34] Y.-K. Peng, Y.-J. Tseng, C.-L. Liu, S.-W. Chou, Y.-W. Chen, S. C. E. Tsang, P.-T. Chou, *Nanoscale* **2015**, *7*, 2676.
- [35] J. G. Croissant, X. Cattoën, M. Wong Chi Man, J.-O. Durand, N. M. Khashab, *Nanoscale* **2015**, *7*, 20318.
- [36] C. Urata, H. Yamada, R. Wakabayashi, Y. Aoyama, S. Hirose, S. Arai, S. Takeoka, Y. Yamauchi, K. Kuroda, *J. Am. Chem. Soc.* **2011**, *133*, 8102.
- [37] S. Datz, H. Engelke, C. v. Schirnding, L. Nguyen, T. Bein, *Microporous Mesoporous Mater.* **2016**, *225*, 371.
- [38] J. Croissant, X. Cattoën, M. W. C. Man, A. Gallud, L. Raehm, P. Trens, M. Maynadier, J.-O. Durand, *Adv. Mater.* **2014**, *26*, 6174.
- [39] Y. Yang, Y. Niu, J. Zhang, A. K. Meka, H. Zhang, C. Xu, C. X. C. Lin, M. Yu, C. Yu, *Small* **2015**, *11*, 2743.
- [40] J. G. Croissant, C. Qi, O. Mongin, V. Hugues, M. Blanchard-Desce, L. Raehm, X. Cattoën, M. Wong Chi Man, M. Maynadier, M. Gary-Bobo, M. Garcia, J. I. Zink, J.-O. Durand, *J. Mater. Chem. B* **2015**, *3*, 6456.
- [41] Y. Chen, Q. Meng, M. Wu, S. Wang, P. Xu, H. Chen, Y. Li, L. Zhang, L. Wang, J. Shi, *J. Am. Chem. Soc.* **2014**, *136*, 16326.
- [42] J. G. Croissant, Y. Fatieiev, K. Julfakyan, J. Lu, A.-H. Emwas, D. H. Anjum, H. Omar, F. Tamanoi, J. I. Zink, N. M. Khashab, *Chem. – A Eur. J.* **2016**, *22*, 14806.
- [43] L. Maggini, L. Travaglini, I. Cabrera, P. Castro-Hartmann, L. De Cola, *Chem. – A Eur. J.* **2016**, *22*, 3697.
- [44] K. Braun, A. Pochert, M. Beck, R. Fiedler, J. Gruber, M. Lindén, *J. Sol-Gel Sci. Technol.* **2016**, *79*, 319.
- [45] X. Huang, N. P. Young, H. E. Townley, *Nanomater. Nanotechnol.* **2014**, *4*, 2.
- [46] Y.-N. Zhang, W. Poon, A. J. Tavares, I. D. McGilvray, W. C. W. Chan, *J. Control. Release* **2016**, *240*, 332.
- [47] M. Beck, T. Mandal, C. Buske, M. Lindén, *ACS Appl. Mater. Interfaces* **2017**, *9*, 18566.
- [48] F. Chen, H. Hong, Y. Zhang, H. F. Valdovinos, S. Shi, G. S. Kwon, C. P. Theuer, T. E. Barnhart, W. Cai, *ACS Nano* **2013**, *7*, 9027.

- [49] S. Goel, F. Chen, H. Hong, H. F. Valdovinos, R. Hernandez, S. Shi, T. E. Barnhart, W. Cai, *ACS Appl. Mater. Interfaces* **2014**, *6*, 21677.
- [50] S. Goel, F. Chen, S. Luan, H. F. Valdovinos, S. Shi, S. A. Graves, F. Ai, T. E. Barnhart, C. P. Theuer, W. Cai, *Adv. Sci. (Weinheim, Baden-Wuerttemberg, Ger.)* **2016**, *3*, 1600122.
- [51] F. Chen, H. F. Valdovinos, R. Hernandez, S. Goel, T. E. Barnhart, W. Cai, *Acta Pharmacol. Sin.* **2017**, *38*, 907.
- [52] Q. He, Z. Zhang, F. Gao, Y. Li, J. Shi, *Small* **2011**, *7*, 271.
- [53] L. Kramer, G. Winter, B. Baur, A. J. Kuntz, T. Kull, C. Solbach, A. J. Beer, M. Lindén, *Nanoscale* **2017**, *9*, 9743.
- [54] L. Miller, G. Winter, B. Baur, B. Witulla, C. Solbach, S. Reske, M. Lindén, *Nanoscale* **2014**, *6*, 4928.
- [55] T. Yu, D. Hubbard, A. Ray, H. Ghandehari, *J. Control. Release* **2012**, *163*, 46.
- [56] J. S. Souris, C.-H. Lee, S.-H. Cheng, C.-T. Chen, C.-S. Yang, J. A. Ho, C.-Y. Mou, L.-W. Lo, *Biomaterials* **2010**, *31*, 5564.
- [57] X. Huang, L. Li, T. Liu, N. Hao, H. Liu, D. Chen, F. Tang, *ACS Nano* **2011**, *5*, 5390.
- [58] D. Shao, M. Lu, Y. Zhao, F. Zhang, Y. Tan, X. Zheng, Y. Pan, X. Xiao, Z. Wang, W. Dong, J. Li, L. Chen, *Acta Biomater.* **2017**, *49*, 531.
- [59] J. Lu, M. Liong, Z. Li, J. I. Zink, F. Tamanoi, *Small* **2010**, *6*, 1794.
- [60] M. A. Malfatti, H. A. Palko, E. A. Kuhn, K. W. Turteltaub, *Nano Lett.* **2012**, *12*, 5532.
- [61] J. Lu, Z. Li, J. I. Zink, F. Tamanoi, *Nanomedicine Nanotechnology, Biol. Med.* **2012**, *8*, 212.
- [62] R. D. Vinluan, J. Zheng, *Nanomedicine* **2015**, *10*, 2781.
- [63] Z. Chen, H. Chen, H. Meng, G. Xing, X. Gao, B. Sun, X. Shi, H. Yuan, C. Zhang, R. Liu, F. Zhao, Y. Zhao, X. Fang, *Toxicol. Appl. Pharmacol.* **2008**, *230*, 364.
- [64] M. Lindén, In *Mesoporous Silica-based Nanomaterials and Biomedical Applications, Part A*; Tamanoi, F. B. T.-T. E., Ed.; Academic Press, 2018; Vol. 43, pp. 155–180.
- [65] V. Cauda, C. Argyo, T. Bein, *J. Mater. Chem.* **2010**, *20*, 8693.
- [66] J. L. Paris, P. D. La Torre, M. Manzano, M. V. Cabañas, A. I. Flores, M. Vallet-Regí, *Acta Biomater.* **2016**, *33*, 275.
- [67] A. Maleki, H. Kettiger, A. Schoubben, J. M. Rosenholm, V. Ambrogio, M. Hamidi, *J. Control. Release* **2017**, *262*, 329.
- [68] M. Vallet-Regí, M. Manzano, J. M. González-Calbet, E. Okunishi, *Chem. Commun.* **2010**, *46*, 2956.
- [69] S. Mura, J. Nicolas, P. Couvreur, *Nat Mater* **2013**, *12*, 991.
- [70] N. Kumar, W. Chen, C.-A. Cheng, T. Deng, R. Wang, J. I. Zink, In *Mesoporous Silica-based Nanomaterials and Biomedical Applications, Part A*; Tamanoi, F. B. T.-T. E., Ed.; Academic Press, 2018; Vol. 43, pp. 31–65.
- [71] M. W. Ambrogio, C. R. Thomas, Y.-L. Zhao, J. I. Zink, J. F. Stoddart, *Acc. Chem. Res.* **2011**, *44*, 903.
- [72] J. E. Lee, N. Lee, T. Kim, J. Kim, T. Hyeon, *Acc. Chem. Res.* **2011**, *44*, 893.
- [73] Z. Li, J. C. Barnes, A. Bosoy, J. F. Stoddart, J. I. Zink, *Chem. Soc. Rev.* **2012**, *41*, 2590.
- [74] J. L. Vivero-Escoto, R. C. Huxford-Phillips, W. Lin, *Chem. Soc. Rev.* **2012**, *41*, 2673.
- [75] Y. Chen, H. Chen, J. Shi, *Adv. Mater.* **2013**, *25*, 3144.
- [76] Z. Tao, *RSC Adv.* **2014**, *4*, 18961.
- [77] V. Biju, *Chem. Soc. Rev.* **2014**, *43*, 744.
- [78] F. Peng, Y. Su, Y. Zhong, C. Fan, S.-T. Lee, Y. He, *Acc. Chem. Res.* **2014**, *47*, 612.
- [79] B. Rühle, P. Saint-Cricq, J. I. Zink, *ChemPhysChem* **2016**, *17*, 1769.
- [80] E. Aznar, M. Oroval, L. Pascual, J. R. Murguía, R. Martínez-Máñez, F. Sancenón, *Chem. Rev.* **2016**, *116*, 561.
- [81] H. Meng, M. Xue, T. Xia, Y.-L. Zhao, F. Tamanoi, J. F. Stoddart, J. I. Zink, A. E. Nel,



- J. Am. Chem. Soc.* **2010**, *132*, 12690.
- [82] Z. Li, D. L. Clemens, B.-Y. Lee, B. J. Dillon, M. A. Horwitz, J. I. Zink, *ACS Nano* **2015**, *9*, 10778.
- [83] S. Angelos, N. M. Khashab, Y.-W. Yang, A. Trabolsi, H. A. Khatib, J. F. Stoddart, J. I. Zink, *J. Am. Chem. Soc.* **2009**, *131*, 12912.
- [84] C. Théron, A. Gallud, C. Carcel, M. Gary-Bobo, M. Maynadier, M. Garcia, J. Lu, F. Tamanoi, J. I. Zink, M. Wong Chi Man, *Chem. – A Eur. J.* **2014**, *20*, 9372.
- [85] Y.-L. Zhao, Z. Li, S. Kabehie, Y. Y. Botros, J. F. Stoddart, J. I. Zink, *J. Am. Chem. Soc.* **2010**, *132*, 13016.
- [86] C. Acosta, E. Pérez-Esteve, C. A. Fuenmayor, S. Benedetti, M. S. Cosio, J. Soto, F. Sancenón, S. Mannino, J. Barat, M. D. Marcos, R. Martínez-Máñez, *ACS Appl. Mater. Interfaces* **2014**, *6*, 6453.
- [87] V. Cauda, C. Argyo, A. Schlossbauer, T. Bein, *J. Mater. Chem.* **2010**, *20*, 4305.
- [88] L. Xing, H. Zheng, Y. Cao, S. Che, *Adv. Mater.* **2012**, *24*, 6433.
- [89] J. Fu, Y. Zhu, Y. Zhao, *J. Mater. Chem. B* **2014**, *2*, 3538.
- [90] J. M. Rosenholm, E. Peuhu, J. E. Eriksson, C. Sahlgren, M. Lindén, *Nano Lett.* **2009**, *9*, 3308.
- [91] Y. Zhu, J. Shi, W. Shen, X. Dong, J. Feng, M. Ruan, Y. Li, *Angew. Chemie Int. Ed.* **2005**, *44*, 5083.
- [92] M. Martínez-Carmona, D. Lozano, M. Colilla, M. Vallet-Regí, *Acta Biomater.* **2018**, *65*, 393.
- [93] K. Patel, S. Angelos, W. R. Dichtel, A. Coskun, Y.-W. Yang, J. I. Zink, J. F. Stoddart, *J. Am. Chem. Soc.* **2008**, *130*, 2382.
- [94] C. Park, H. Kim, S. Kim, C. Kim, *J. Am. Chem. Soc.* **2009**, *131*, 16614.
- [95] N. Singh, A. Karambelkar, L. Gu, K. Lin, J. S. Miller, C. S. Chen, M. J. Sailor, S. N. Bhatia, *J. Am. Chem. Soc.* **2011**, *133*, 19582.
- [96] L. Mondragón, N. Mas, V. Ferragud, C. de la Torre, A. Agostini, R. Martínez-Máñez, F. Sancenón, P. Amorós, E. Pérez-Payá, M. Orzáez, *Chem. – A Eur. J.* **2014**, *20*, 5271.
- [97] K. Radhakrishnan, S. Gupta, D. P. Gnanadhas, P. C. Ramamurthy, D. Chakravorty, A. M. Raichur, *Part. Part. Syst. Character.* **2013**, *31*, 449.
- [98] Y.-J. Cheng, G.-F. Luo, J.-Y. Zhu, X.-D. Xu, X. Zeng, D.-B. Cheng, Y.-M. Li, Y. Wu, X.-Z. Zhang, R.-X. Zhuo, F. He, *ACS Appl. Mater. Interfaces* **2015**, *7*, 9078.
- [99] S. H. van Rijt, D. A. Bölükbas, C. Argyo, S. Datz, M. Lindner, O. Eickelberg, M. Königshoff, T. Bein, S. Meiners, *ACS Nano* **2015**, *9*, 2377.
- [100] B. Kumar, S. Kulanthaivel, A. Mondal, S. Mishra, B. Banerjee, A. Bhaumik, I. Banerjee, S. Giri, *Colloids Surfaces B Biointerfaces* **2017**, *150*, 352.
- [101] B. Ruehle, D. L. Clemens, B.-Y. Lee, M. A. Horwitz, J. I. Zink, *J. Am. Chem. Soc.* **2017**, *139*, 6663.
- [102] R. Bhat, I. García, E. Aznar, B. Arnaiz, M. C. Martínez-Bisbal, L. M. Liz-Marzán, S. Penadés, R. Martínez-Máñez, *Nanoscale* **2018**, *10*, 239.
- [103] T. D. Nguyen, H.-R. Tseng, P. C. Celestre, A. H. Flood, Y. Liu, J. F. Stoddart, J. I. Zink, *Proc. Natl. Acad. Sci. U. S. A.* **2005**, *102*, 10029.
- [104] T. D. Nguyen, Y. Liu, S. Saha, K. C.-F. Leung, J. F. Stoddart, J. I. Zink, *J. Am. Chem. Soc.* **2007**, *129*, 626.
- [105] M. W. Ambrogio, T. A. Pecorelli, K. Patel, N. M. Khashab, A. Trabolsi, H. A. Khatib, Y. Y. Botros, J. I. Zink, J. F. Stoddart, *Org. Lett.* **2010**, *12*, 3304.
- [106] X. Ma, K. T. Nguyen, P. Borah, C. Y. Ang, Y. Zhao, *Adv. Healthc. Mater.* **2012**, *1*, 690.
- [107] J. Zhang, M. Niemelä, J. Westermarck, J. M. Rosenholm, *Dalt. Trans.* **2014**, *43*, 4115.
- [108] F. Porta, G. E. M. Lamers, J. I. Zink, A. Kros, *Phys. Chem. Chem. Phys.* **2011**, *13*, 9982.

- [109] N. M. Khashab, A. Trabolsi, Y. A. Lau, M. W. Ambrogio, D. C. Friedman, H. A. Khatib, J. I. Zink, J. F. Stoddart, *European J. Org. Chem.* **2009**, 2009, 1669.
- [110] P. Nadrah, F. Porta, O. Planinšek, A. Kros, M. Gaberšček, *Phys. Chem. Chem. Phys.* **2013**, *15*, 10740.
- [111] B.-Y. Lee, Z. Li, D. L. Clemens, B. J. Dillon, A. A. Hwang, J. I. Zink, M. A. Horwitz, *Small* **2016**, *12*, 3690.
- [112] P. Shi, Y. Qu, C. Liu, H. Khan, P. Sun, W. Zhang, *ACS Macro Lett.* **2016**, *5*, 88.
- [113] C. R. Thomas, D. P. Ferris, J.-H. Lee, E. Choi, M. H. Cho, E. S. Kim, J. F. Stoddart, J.-S. Shin, J. Cheon, J. I. Zink, *J. Am. Chem. Soc.* **2010**, *132*, 10623.
- [114] P. Saint-Cricq, S. Deshayes, J. I. Zink, A. M. Kasko, *Nanoscale* **2015**, *7*, 13168.
- [115] B. Rühle, S. Datz, C. Argyo, T. Bein, J. I. Zink, *Chem. Commun.* **2016**, 52, 1843.
- [116] Y. Zhu, C. Tao, *RSC Adv.* **2015**, *5*, 22365.
- [117] A. Baeza, E. Guisasola, E. Ruiz-Hernández, M. Vallet-Regí, *Chem. Mater.* **2012**, *24*, 517.
- [118] E. Bringas, Ö. Köysüren, D. V Quach, M. Mahmoudi, E. Aznar, J. D. Roehling, M. D. Marcos, R. Martínez-Máñez, P. Stroeve, *Chem. Commun.* **2012**, 48, 5647.
- [119] B. Chang, J. Guo, C. Liu, J. Qian, W. Yang, *J. Mater. Chem.* **2010**, *20*, 9941.
- [120] P.-J. Chen, S.-H. Hu, C.-S. Hsiao, Y.-Y. Chen, D.-M. Liu, S.-Y. Chen, *J. Mater. Chem.* **2011**, *21*, 2535.
- [121] J. L. Paris, M. V. Cabanas, M. Manzano, M. Vallet-Regí, *ACS Nano* **2015**, *9*, 11023.
- [122] J. L. Paris, M. Manzano, V. Cabañas, M. Vallet-Regí, *Nanoscale* **2018**, *10*, 6402.
- [123] Y. Lv, Y. Cao, P. Li, J. Liu, H. Chen, W. Hu, L. Zhang, *Adv. Healthc. Mater.* **2017**, *6*, 1700354.
- [124] X. Li, C. Xie, H. Xia, Z. Wang, *Langmuir* **2018**, *34*, 9974.
- [125] J. Wang, Y. Jiao, Y. Shao, *Mater. (Basel, Switzerland)* **2018**, *11*, 2041.
- [126] P. Sierocki, H. Maas, P. Dragut, G. Richardt, F. Vögtle, L. De Cola, F. Brouwer, J. I. Zink, *J. Phys. Chem. B* **2006**, *110*, 24390.
- [127] Y. Zhu, M. Fujiwara, *Angew. Chemie-International Ed.* **2007**, *46*, 2241.
- [128] J. Lu, E. Choi, F. Tamanoi, J. I. Zink, *Small* **2008**, *4*, 421.
- [129] D. P. Ferris, Y.-L. Zhao, N. M. Khashab, H. A. Khatib, J. F. Stoddart, J. I. Zink, *J. Am. Chem. Soc.* **2009**, *131*, 1686.
- [130] D. Tarn, D. P. Ferris, J. C. Barnes, M. W. Ambrogio, J. F. Stoddart, J. I. Zink, *Nanoscale* **2014**, *6*, 3335.
- [131] D. Wang, S. Wu, *Langmuir* **2016**, *32*, 632.
- [132] A. Agostini, F. Sancenón, R. Martínez-Máñez, M. D. Marcos, J. Soto, P. Amorós, *Chem. – A Eur. J.* **2012**, *18*, 12218.
- [133] J. Lai, X. Mu, Y. Xu, X. Wu, C. Wu, C. Li, J. Chen, Y. Zhao, *Chem. Commun.* **2010**, 46, 7370.
- [134] Z. Zhang, L. Wang, J. Wang, X. Jiang, X. Li, Z. Hu, Y. Ji, X. Wu, C. Chen, *Adv. Mater.* **2012**, *24*, 1418.
- [135] J. G. Croissant, J.-O. Durand, In *Mesoporous Silica-based Nanomaterials and Biomedical Applications, Part A*; Tamanoi, F. B. T.-T. E., Ed.; Academic Press, 2018; Vol. 43, pp. 67–99.
- [136] Q. Lin, Q. Huang, C. Li, C. Bao, Z. Liu, F. Li, L. Zhu, *J. Am. Chem. Soc.* **2010**, *132*, 10645.
- [137] J. S. Robbins, K. M. Schmid, S. T. Phillips, *J. Org. Chem.* **2013**, *78*, 3159.
- [138] W. Ji, N. Li, D. Chen, X. Qi, W. Sha, Y. Jiao, Q. Xu, J. Lu, *J. Mater. Chem. B* **2013**, *1*, 5942.
- [139] M. Gary-Bobo, Y. Mir, C. Rouxel, D. Brevet, I. Basile, M. Maynadier, O. Vaillant, O. Mongin, M. Blanchard-Desce, A. Morère, M. Garcia, J.-O. Durand, L. Raehm, *Angew. Chemie* **2011**, *123*, 11627.

- [140] T. M. Guardado-Alvarez, L. Sudha Devi, M. M. Russell, B. J. Schwartz, J. I. Zink, *J. Am. Chem. Soc.* **2013**, *135*, 14000.
- [141] J. G. Croissant, O. Mongin, V. Hugues, M. Blanchard-Desce, X. Cattoën, M. Wong Chi Man, V. Stojanovic, C. Charnay, M. Maynadier, M. Gary-Bobo, M. Garcia, L. Raehm, J.-O. Durand, *J. Mater. Chem. B* **2015**, *3*, 5182.
- [142] J. Dong, M. Xue, J. I. Zink, *Nanoscale* **2013**, *5*, 10300.
- [143] H. Liu, Y. Yang, A. Wang, M. Han, W. Cui, J. Li, *Adv. Funct. Mater.* **2016**, *26*, 2561.
- [144] J. G. Croissant, S. Picard, D. Aggad, M. Klausen, C. Mauriello Jimenez, M. Maynadier, O. Mongin, G. Clermont, E. Genin, X. Cattoën, M. Wong Chi Man, L. Raehm, M. Garcia, M. Gary-Bobo, M. Blanchard-Desce, J.-O. Durand, *J. Mater. Chem. B* **2016**, *4*, 5567.
- [145] V. Mamaeva, J. M. Rosenholm, L. T. Bate-Eya, L. Bergman, E. Peuhu, A. Duchanoy, L. E. Fortelius, S. Landor, D. M. Toivola, M. Lindén, C. Sahlgren, *Mol. Ther.* **2011**, *19*, 1538.
- [146] X. Wang, X. Li, A. Ito, Y. Sogo, T. Ohno, *Acta Biomater.* **2013**, *9*, 7480.
- [147] Y. Zhao, X. Sun, G. Zhang, B. G. Trewyn, I. I. Slowing, V. S.-Y. Lin, *ACS Nano* **2011**, *5*, 1366.
- [148] L. Li, T. Liu, C. Fu, L. Tan, X. Meng, H. Liu, *Nanomedicine Nanotechnology, Biol. Med.* **2015**, *11*, 1915.
- [149] H. Maeda, H. Nakamura, J. Fang, *Adv. Drug Deliv. Rev.* **2013**, *65*, 71.
- [150] J. Kim, H. S. Kim, N. Lee, T. Kim, H. Kim, T. Yu, I. C. Song, W. K. Moon, T. Hyeon, *Angew. Chemie Int. Ed.* **2008**, *47*, 8438.
- [151] H. Meng, M. Xue, T. Xia, Z. Ji, D. Y. Tarn, J. I. Zink, A. E. Nel, *ACS Nano* **2011**, *5*, 4131.
- [152] Y. Nakamura, A. Mochida, P. L. Choyke, H. Kobayashi, Nanodrug Delivery: Is the Enhanced Permeability and Retention Effect Sufficient for Curing Cancer? *Bioconjug. Chem.* **2016**, *27*, 2225–2238.
- [153] C. Chen, J. Ke, X. E. Zhou, W. Yi, J. S. Brunzelle, J. Li, E.-L. Yong, H. E. Xu, K. Melcher, *Nature* **2013**, *500*, 486.
- [154] P. Khosravian, M. Shafiee Ardestani, M. Khoobi, S. N. Ostad, F. A. Dorkoosh, H. Akbari Javar, M. Amanlou, *Onco. Targets. Ther.* **2016**, *9*, 7315.
- [155] F. Porta, G. E. M. Lamers, J. Morrhayim, A. Chatzopoulou, M. Schaaf, H. den Dulk, C. Backendorf, J. I. Zink, A. Kros, *Adv. Healthc. Mater.* **2013**, *2*, 281.
- [156] Q. Zhang, X. Wang, P.-Z. Li, K. T. Nguyen, X.-J. Wang, Z. Luo, H. Zhang, N. S. Tan, Y. Zhao, *Adv. Funct. Mater.* **2014**, *24*, 2450.
- [157] M. K. Gurka, D. Pender, P. Chuong, B. L. Fouts, A. Sobelov, M. W. McNally, M. Mezera, S. Y. Woo, L. R. McNally, *J. Control. Release* **2016**, *231*, 60.
- [158] G. Villaverde, A. Baeza, G. J. Melen, A. Alfranca, M. Ramirez, M. Vallet-Regí, *J. Mater. Chem. B* **2015**, *3*, 4831.
- [159] R. R. Castillo, D. Lozano, M. Vallet-Regí, *Bioconjug. Chem.* **2018**, *29*, 3677.
- [160] G. Villaverde, A. Alfranca, Á. Gonzalez-Murillo, G. J. Melen, R. R. Castillo, M. Ramirez, A. Baeza, M. Vallet-Regí, *Angew. Chemie Int. Ed.* **2019**, *58*, 3067.
- [161] P. A. Netti, D. A. Berk, M. A. Swartz, A. J. Grodzinsky, R. K. Jain, *Cancer Res.* **2000**, *60*, 2497.
- [162] A. Parodi, S. G. Haddix, N. Taghipour, S. Scaria, F. Taraballi, A. Cevenini, I. K. Yazdi, C. Corbo, R. Palomba, S. Z. Khaled, J. O. Martinez, B. S. Brown, L. Isenhardt, E. Tasciotti, *ACS Nano* **2014**, *8*, 9874.
- [163] M. R. Villegas, A. Baeza, M. Vallet-Regí, *ACS Appl. Mater. Interfaces* **2015**, *7*, 24075.
- [164] J. L. Paris, C. Mannaris, M. V. Cabañas, R. Carlisle, M. Manzano, M. Vallet-Regí, C. C. Coussios, *Chem. Eng. J.* **2018**, *340*, 2.